

Synthesis and Characterization of Ternary Zinc–Antimony–Transition Metal Spinel

D. Poleti¹ and D. Vasović

Department of General and Inorganic Chemistry, Faculty of Technology and Metallurgy, University of Belgrade, P.O. Box 494, 11001 Belgrade, Yugoslavia

Lj. Karanović

Crystallographic Laboratory, Faculty of Mining and Geology, University of Belgrade, P.O. Box 162, 11001 Belgrade, Yugoslavia

and

Z. Branković

Institute of Technical Sciences of the Serbian Academy of Sciences and Arts, Knez Mihailova 35, 11000 Belgrade, Yugoslavia

Received May 3, 1993; in revised form October 21, 1993; accepted October 25, 1993

Four series of ternary $Zn_xMe_ySb_zO_4$ spinels, $Me = Cr, Mn, Co,$ or Ni , $y \leq 0.778$, have been prepared by solid state reaction from appropriate oxides. The spinels were characterized by the X-ray powder diffraction method. The efficiency of Me ions to form spinel structure measured by the temperature needed to obtain the pure spinel phase decreases in the order $Cr \approx Mn > Co > Ni$. The reaction temperature also becomes lower with increasing content of Me ions. The spinel lattice constants decrease linearly with increasing Me content, while the slope of curves depends on the ionic radii of Me ions. These results allow the lattice constant of more complex spinels to be estimated.

Crystal structures of $(Zn_{1.000})[Zn_{0.633}Co_{0.700}Sb_{0.667}]O_4$, $a = 0.85822(1)$ nm, and $(Zn_{1.000})[Zn_{0.816}Cr_{0.778}Sb_{0.407}]O_4$, $a = 0.84924(1)$ nm, spinels, where () denotes tetrahedral and [] octahedral sites, are determined by Rietveld's method from X-ray powder diffraction data. The results show that Co(II), Cr(III), and Sb(V) are situated in the octahedral site. The tetrahedral site is occupied exclusively by Zn ions. The same cation distribution was postulated for all spinels. © 1994 Academic Press, Inc.

INTRODUCTION

A large group of compounds with the general formula AB_2X_4 , where A and B are different cations and X is an anion (usually oxygen), crystallize with the spinel (Sp) structure. These compounds are important not only as naturally occurring minerals, but also in many branches of solid state science.

¹ To whom correspondence should be addressed.

Mixed oxides with Sp structure have very wide and diverse applications. They are known as pigments with high thermal and chemical stability suitable for coloring enamels and ceramics (1). Also, some Sp-type compounds are excellent refractory (2), magnetic (3), and catalytic materials (4, 5).

There are examples where Sp are components of some composite, multiphase systems. One such example is zinc oxide-based varistor ceramic which contains more than 10 mass% of Sp phase (6). Varistors are semiconductor electrical devices with nonlinear current–voltage characteristics having application as circuit protectors against transients and power overloads (7). The varistors are made by high-temperature ($\geq 1200^\circ\text{C}$) sintering ZnO with small quantities of additives like oxides of Bi, Sb, Mn, Cr, Co, Ni, Si, and some other metals. The microstructure of varistors comprises ZnO grains, intergranular Bi_2O_3 -rich phase, and Sp phase. In some cases a pyrochlore phase appears, as a minor constituent (8).

Because of system complexity the role of Sp phase in varistors is not very well understood. Possibly, the presence of Sp has an inhibiting effect on ZnO grain growth, thus raising the breakdown voltage of varistors (8). It is also assumed (9) that Sp phase interrupts the network of Bi_2O_3 -rich phase, preventing the bypass current effect, which may degrade the nonlinearity.

There is general agreement that the formula of Sp phase in varistor ceramics is approximately $Zn_{2.333}Sb_{0.667}O_4$ (6, 10). However, this phase generally dissolves the other elements present in the system. For example, for a varistor system containing Bi_2O_3 , Sb_2O_3 , CoO, MnO, Cr_2O_3 ,

and SiO₂, as additives, it is suggested that all of Sb₂O₃, one-fourth of CoO, two-thirds of MnO, and five-sixths of Cr₂O₃ added go into Sp phase (9). In the system containing NiO instead of SiO₂ (6), an electron-probe microanalysis showed the following composition of Sp phase: ZnO, 48–54.5%; Sb₂O₃, 33–35%; Cr₂O₃, 6–8%; MnO₂, 2.5–3%; CoO, 1–1.5%; and NiO, 4–5% (the actual percentage depends on sintering conditions). Very similar composition was also reported by B  ther and co-workers (11).

Structural characteristics of Sp phase in varistors are not investigated in detail. It has been shown that the unit cell of Sp phase in real varistor samples is always smaller than the unit cell of Zn_{2.333}Sb_{0.667}O₄ (10–12).

In the present work, a systematic study of the ternary zinc–antimony-based spinels, where Zn or Zn and Sb are partially substituted by Cr, Mn, Co, or Ni ions, is

described. In addition, crystal structures of (Zn_{1.000}) [Zn_{0.633}Co_{0.700}Sb_{0.667}]O₄ and (Zn_{1.000})[Zn_{0.816}Cr_{0.778}Sb_{0.407}]O₄ spinels, where () denotes tetrahedral and [] octahedral sites, are determined by Rietveld's method from X-ray powder diffraction (XRD) data.

EXPERIMENTAL

Sample Preparation and Characterization

Besides the parent Zn_{2.333}Sb_{0.667}O₄ spinel, four series of spinels with formula Zn_xMe_ySb_zO₄, where Me = Cr, Mn, Co, or Ni, have been prepared. Each series included three samples with gradually increasing content of Me ions (Table 1). In accordance with analytical data briefly discussed in the Introduction, Zn substitution was limited up to 30

TABLE 1
Composition, Final Synthetic Conditions, and Properties of Spinel

Formula	Thermal treatment, <i>t</i> (°C)/ <i>τ</i> (h) ^a	Color ^b	Lattice parameter	
			<i>a</i> _{obs} (nm)	<i>a</i> _{calc} ^c (nm)
Zn _{2.333} Sb _{0.667} O ₄	900/3	White	0.8594(1)	0.8594
Zn _{2.171} Cr _{0.241} Sb _{0.586} O ₄	1100/3	Green	0.8564(1)	0.8555
Zn _{2.000} Cr _{0.500} Sb _{0.500} O ₄	1100/3	Green	0.85259(7)	0.8526
Zn _{1.815} Cr _{0.778} Sb _{0.407} O ₄	1100/3	Green	0.8493(2) ^d	0.8488
Zn _{2.171} Mn _{0.241} Sb _{0.586} O ₄	1100/3	Brown	0.8573(1)	0.8574
Zn _{2.000} Mn _{0.500} Sb _{0.500} O ₄	1100/3	Brown	0.8548(2)	0.8565
Zn _{1.815} Mn _{0.778} Sb _{0.407} O ₄	1100/3	Brown	0.8547(1) ^e	0.8549
	1150/3		0.8554(3) ^e	
	1150/6		0.85683(4) ^e	
Zn _{2.100} Co _{0.233} Sb _{0.667} O ₄	1200/3	Brown	0.8595(2)	0.8589
				0.8593 ^f
Zn _{1.867} Co _{0.467} Sb _{0.667} O ₄	1150/8	Brown	0.8587(2)	0.8587
				0.8592 ^f
Zn _{1.633} Co _{0.700} Sb _{0.667} O ₄	1150/8	Brown	0.8583(2) ^d	0.8580
				0.8591 ^f
Zn _{2.100} Ni _{0.233} Sb _{0.667} O ₄	1200/3	Yellow-Green	0.8584(2)	0.8577
				0.8594 ^f
Zn _{1.867} Ni _{0.467} Sb _{0.667} O ₄	1200/3	Yellow-Green	0.8573(1)	0.8563
				0.8594 ^f
Zn _{1.633} Ni _{0.700} Sb _{0.667} O ₄	1150/3	Brown-Green	0.8548(3)	0.8543
				0.8594 ^f
Zn _{1.991} Ni _{0.090} Co _{0.030} Cr _{0.247} Mn _{0.090} Sb _{0.545} O ₄	1100/3	Brown	0.8546(1)	0.8530

^a Only the final values are listed (for explanation see Experimental).

^b With increasing content of transition metal the color becomes darker.

^c Lattice parameters calculated using "cation–anion" distances given by Poix (15, 16). The tetrahedral site is occupied exclusively by Zn ions.

^d Structural investigations using X-ray powder diffraction data were performed.

^e The pure Sp phase was not obtained.

^f Lattice parameters calculated as given in footnote c. The tetrahedral site is occupied by Co + Zn or Ni + Zn ions.

mole%. Formulas of spinels were calculated in accordance with atomic,

$$x + y + z = 3,$$

and charge balance;

$$2x + 2y + 5z = 8 \quad (\text{for Co and Ni spinels})$$

$$2x + 3y + 5z = 8 \quad (\text{for Cr spinels}).$$

It is known that Mn in Sp structures can exist in various oxidation states (13). Preliminary investigation of Mn spinels showed that, no matter what initial stoichiometry was chosen, its unit cells are smaller than the unit cell of the parent spinel. Considering ionic radii of Zn^{2+} and different Mn^{n+} ions (14) such behavior is possible only if Mn occurs as Mn^{3+} , Mn^{4+} , or the mixture of both ions. The presence of Mn^{3+} ions was postulated and the formulas of Mn spinels are calculated in the same manner as the formulas of Cr spinels.

One complex spinel with formula $\text{Zn}_{1.991}\text{Ni}_{0.090}\text{Co}_{0.030}\text{Cr}_{0.247}\text{Mn}_{0.090}\text{Sb}_{0.545}\text{O}_4$ was also synthesized for comparison.

The samples are prepared from the following oxides: ZnO , Sb_2O_3 , Cr_2O_3 , MnO_2 , Co_3O_4 , and NiO , all of reagent-grade quality. The oxides in appropriate molar ratio (for 3 g of sample) are homogenized by dry milling in agate mortar for 0.5 hr. Thermal treatment was as follows:

the samples in platinum or porcelain crucible were put in the cool furnace, heated in air up to 1100°C , kept 3 hr at this temperature, and furnace cooled. The samples were then examined by the X-ray powder diffraction technique on a Philips PW 710 automatic diffractometer using monochromated $\text{CuK}\alpha$ radiation. If the pure Sp was not obtained the heating time was first prolonged and then the temperature was raised.

Synthetic conditions, color, and lattice parameters of spinels are listed in Table 1.

The lattice constants were calculated by least-square technique (Program LSUCRIPC) (17).

XRD Data Collection and Structure Refinements

Experimental conditions and crystal data for the spinels investigated are listed in Table 2.

The refinements were made by Rietveld's method (18) using the DBWS-9006PC program (19) on an IBM PC AT compatible computer. The program minimizes the function $\sum w_i(y_{io} - y_{ic})^2$, where y_{io} and y_{ic} are the observed and calculated data points and $w_i = 1/y_{io}$. The data are not corrected for absorption and extinction. Preferred orientation is not detected. Peaks below $40^\circ 2\theta$ are corrected for asymmetry. Background was refined as a four-parameter function.

Structures of Co_3O_4 and NiCo_2O_4 spinels (20) were taken as the starting model: Zn1 is fixed at $\frac{1}{8}$, $\frac{1}{8}$, $\frac{1}{8}$ (8a position), Zn2 and the other metal ions are fixed at $\frac{1}{2}$, $\frac{1}{2}$,

TABLE 2
Experimental Conditions and Crystal Data for $(\text{Zn}_{1.000})[\text{Zn}_{0.633}\text{Co}_{0.700}\text{Sb}_{0.667}]\text{O}_4$
and $(\text{Zn}_{1.000})[\text{Zn}_{0.815}\text{Cr}_{0.778}\text{Sb}_{0.407}]\text{O}_4$ Spinel

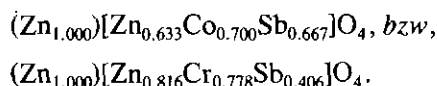
	Co spinel	Cr spinel
Diffractometer	PW1710	
X-ray tube	Cu LFF, 40 kV, 30 mA	
Wavelength (nm)	0.15405, 0.15443	
Profile range ($^\circ 2\theta$)	10–120	
Step width ($^\circ 2\theta$)	0.025	
Step time (s)	5	
Peak range (number of FWHM) ^a	12.0	
Number of observations	4400	
Number of maxima in the examined 2θ range	70	69
Space group	$Fd\bar{3}m$, No. 227 (origin at center $\bar{3}m$)	
a (nm)	0.85822(1)	0.84924(1)
$R_{\text{exp}} (=100 \cdot [(N - P)/\sum w_i y_{io}^2]^{1/2})$	9.17	8.88
$R_p (=100 \cdot \sum y_{io} - y_{ic} /y_{io})$	11.17	9.41
$R_{\text{wp}} (=100 \cdot [\sum w_i (y_{io} - y_{ic})^2 / \sum w_i y_{io}^2]^{1/2})$	14.94	13.74
$R_B (=100 \cdot \sum I_o - I_c / \sum I_o)$	4.15	3.60
$R_F (=100 \cdot \sum F_o - F_c / \sum F_o)$	3.22	3.21

^a FWHM is the full width at half-maximum of individual reflections and is given by a second-degree polynomial of the form $\text{FWHM}^2 = U \tan^2 \theta + V \tan \theta + W$, where U , V , and W are empirical parameters to be refined in addition to the structural parameters and a background function.

TABLE 3
Final Atomic Coordinates, Isotropic Thermal Parameters, and
Metal–Oxygen Distances (nm)

	x	y	z	B ($\times 10^2$ nm ²)
(Zn _{1.000})[Zn _{0.633} Co _{0.700} Sb _{0.667}]O ₄ , a = 0.85822(1) nm				
O	0.2587(3)	0.2587(3)	0.2587(3)	0.74(9)
Zn1	0.1250	0.1250	0.1250	0.69(4)
Zn2	0.5000	0.5000	0.5000	0.68(3)
Co	0.5000	0.5000	0.5000	0.68(3)
Sb	0.5000	0.5000	0.5000	0.68(3)
Me–O distances				
Tetrahedral				0.1992
Octahedral				0.2071
(Zn _{1.000})[Zn _{0.815} Cr _{0.778} Sb _{0.407}]O ₄ , a = 0.84924(1) nm				
O	0.2593(2)	0.2593(2)	0.2593(2)	0.58(7)
Zn1	0.1250	0.1250	0.1250	0.52(3)
Zn2	0.5000	0.5000	0.5000	0.50(2)
Cr	0.5000	0.5000	0.5000	0.50(2)
Sb	0.5000	0.5000	0.5000	0.50(2)
Me–O distances				
Tetrahedral				0.1971
Octahedral				0.2050

$\frac{1}{2}$ (16d position), while coordinates of O atoms (u , u , u ; position 32e) are varied with starting value 0.25. Occupation numbers were determined according to the formula



Two profile shape functions, pseudo-Voigt and Pearson VII, are tested during refinement and both gave very similar R values. Results presented in Table 2 are for the pseudo-Voigt function. The functions are 46.8 and 47.2% Lorentzian for Co and Cr spinels, respectively.

A total of 17 parameters were varied in the last cycle of refinement ($\Delta/\sigma < 0.05$). Final atomic coordinates, isotropic thermal parameters, and Me–O distances are summarized in Table 3.

After refinement several very weak peaks ($I < 2.0\%$) with d values of 0.2940, 0.2509, 0.2347, 0.1601, and 0.1472 nm are located in the pattern of the Cr spinel. These peaks can be attributed to the trace of another Sp phase.

RESULTS AND DISCUSSION

Stability and Lattice Constants of Spinel Phases

The data listed in Table 1 show that the mixed oxides with Sp structure are obtained in nearly all cases. The only exception is the sample with nominal composition Zn_{1.815}Mn_{0.778}Sb_{0.407}O₄. In contrast to the two Mn spinels with lower Mn content this sample contains a small

amount of Mn₂Sb₂O₇ phase. The peak intensities of Mn₂Sb₂O₇ phase gradually decrease from $I_{\max} = 3.0\%$ to $I_{\max} = 1.6\%$ with prolonged heat treatment. At the same time, an increase of the Sp lattice parameter was observed. Although not investigated in detail, such behavior could be explained by formation of a different Sp phase with the formula Zn_{1.815}Mn_p²⁺Mn_q³⁺Sb_{0.4}O₄.

The pure Zn_{2.333}Sb_{0.667}O₄ appears in two crystal modifications (21). According to Kasper (21) the compound Zn_{2.333}Sb_{0.667}O₄ with Sp structure was prepared at 900°C. Its lattice parameter (Table 1) is in agreement with the Kaspers value (0.8597 nm), but it is higher than the value given in JCPDS file card 15-687 ($a = 0.8585$ nm; 22). The orthorhombic form named β -Zn_{2.333}Sb_{0.667}O₄ is stable between 960 and 1260°C. The cubic, i.e., spinel form, is stable below and above this range (21). In the present investigation the β -modification appeared only in the samples Zn_{2.100}Co_{0.233}Sb_{0.667}O₄, Zn_{2.100}Ni_{0.233}Sb_{0.667}O₄, and Zn_{1.867}Ni_{0.467}Sb_{0.667}O₄ heated at 1100 and 1150°C. It is evident (Table 1) that all ternary spinels were obtained within the range of stability of β -Zn_{2.333}Sb_{0.667}O₄. These observations confirm Inada's conclusion (12) that dissolved ions stabilize Sp modification of Zn_{2.333}Sb_{0.667}O₄. This also explains why β -modification is never observed in the real varistor samples.

The data (Table 1) show that the temperature needed for the complete reaction is lowered with increasing content of Me ions. However, the efficiency of transition metals decreases in the order Cr \approx Mn > Co > Ni, i.e. the more charged and smaller ions are more efficient. The introduction of only 0.029 mol of Cr³⁺ ions into the parent spinel (in an additional experiment) also yielded the pure Sp phase already at 1100°C. Therefore, it seems that Cr³⁺ ion has the greatest stabilizing effect in the systems examined.

Lattice parameters of Sp phases are shown in Fig. 1. Values of a and their changes within individual series for Ni, Mn, and Cr spinels are in accordance with ionic radii (14–16, 23).

Shannon's ionic radius for Co²⁺ is bigger than the radius of Zn²⁺ (0.0745 vs 0.074 nm, respectively) (14). However, our experimental results indicate that Shannon's ionic radius for Co²⁺ is not valid for Sp-type structures. This is in agreement with other authors' data (15, 16, 23).

With the exception of the sample with nominal composition Zn_{1.815}Mn_{0.778}Sb_{0.407}O₄ (see above) all experimental values of a lie on the straight line (Fig. 1). The correlation coefficients (R) obtained by linear regression analysis are better than 0.97 for Mn, Ni, and Cr spinels. The value of R is somewhat smaller (0.92) for Co spinels. This is probably due to the very close values for Zn and Co ionic radii.

Calculated lattice constant ($a = 0.8512$ nm) for Zn_{1.000}Ni_{1.333}Sb_{0.667}O₄ spinel, derived by extrapolation of our experimental data shows reasonable fit with the re-

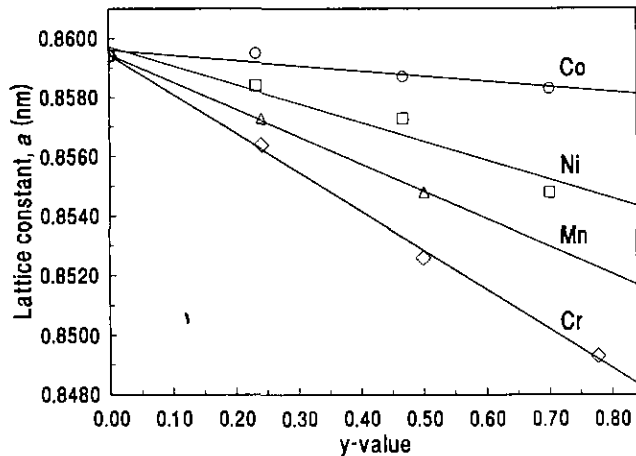


FIG. 1. Lattice parameters of spinels $Zn_xMe_ySb_2O_4$ ($Me=Cr, Mn, Co, \text{ and } Ni$). The data for the sample with a nominal composition $Zn_{1.815}Mn_{0.778}Sb_{0.407}O_4$ (Table 1) are not included.

ported value $a = 0.8516$ nm (21). Also, the estimated value $a = 0.8593$ nm for the spinel $Zn_{2.167}Co_{0.167}Sb_{0.667}O_4$ agrees well with the value $a = 0.8590$ nm published earlier (21).

Structures of $(Zn_{1.000})[Zn_{0.633}Co_{0.700}Sb_{0.667}]O_4$ and $(Zn_{1.000})[Zn_{0.815}Cr_{0.778}Sb_{0.407}]O_4$ Spinels

Because of its completed d -shell (d^{10} electronic configuration) cation Zn^{2+} has no ligand field stabilization energy (24). However, it has been shown (25–27) that the Zn^{2+} ion in spinels has very large tetrahedral site preference. On the other hand, practically all Cr(III) compounds are hexacoordinate with octahedral geometry (28) and Cr^{3+} ion has the largest octahedral site preference of the considered ions in Sp structures. The ions Mn^{3+} and Ni^{2+} also have relatively high octahedral site preference energy. However, Co^{2+} belongs to the ions with small octahedral site preference (25, 27), or even to the ions with tetrahedral site preference (26). To our knowledge, site preference energy of Sb(V) species has not been investigated. However, in all antimony(V)–oxygen systems SbO_6 octahedra were found (29).

From the preceding discussion it follows that the total occupancy of tetrahedral sites by Zn^{2+} ions could be expected with a high probability in all Mn, Cr, and Ni spinels and with a low probability in Co spinels. Thus, Co and Cr spinels are the end members in the series and it was reasonable to choose them for more detailed crystallographic investigation.

The results of structure refinement are listed in Table 3.

In the normal $Me^{2+}Me_2^{3+}O_4$ spinel, 32 oxygen anions and 24 (8 + 16) cations form the unit cell. Oxygen anions for the coordinate $u = 0.25$ build up a cubic close packed array and a regular tetrahedral coordination polyhedron about an $8a$ site and a regular octahedron about a $16d$ site

(23, 30). In this case the octahedral cation–anion distance is 1.155 times larger than the corresponding tetrahedral distance. As u increases, the oxygens displace along the [111] direction, causing the tetrahedral site to enlarge at the expense of the octahedral site. The cation–anion distances, d , are given by (23)

$$d_{tet} = a\sqrt{3}(u - \frac{1}{8})$$

$$d_{oct} = a(3u^2 - 2u + \frac{3}{8})^{1/2}.$$

In our examples, calculated d_{tet} and d_{oct} are 0.1987 and 0.2074 nm for Co spinel and 0.1975 and 0.2047 nm for Cr spinel. These values are in good agreement with experimental values given in Table 3.

The coordinates of O atoms (Table 3) are close to the values found in some $Mn_{1+2x}Cr_{2-3x}Sb_xO_4$ ($0.05 \leq x \leq 0.30$) spinels (31) and in $NiCo_2O_4$ (21). They are also identical within 3σ limits. Therefore, the decreasing of lattice parameters reflects the decreasing of the Me–O distances in tetrahedral and octahedral sites. In the case of Cr spinel the Me–O distances correspond to the values given by Poix (15, 16) (d_{oct} calculated as the mean value for the present ions). For Co spinel the observed d_{tet} is longer and d_{oct} is shorter than the calculated value.

Cation Distribution

The cation distribution was checked in the course of the crystal structure refinement. The XRD data for Cr spinel clearly confirmed the presence of Cr^{3+} and Sb^V species in the octahedral sites. The other combinations of site occupancy yielded nonpositive definite thermal parameters of some ions.

The cation distribution in Co spinel was tested in two ways. If the occupation numbers are fixed in accordance with the formula $(Zn_{0.300}Co_{0.700})[Zn_{1.333}Sb_{0.667}]O_4$ somewhat higher R_p and R_{wp} values (12.87 and 16.70%) and much higher R_B and R_F (9.30 and 6.01%) were obtained after refinement. On the other hand, when occupation numbers are varied during refinement, least squares converged with tetrahedral site totally occupied with Zn^{2+} ions. Both results confirm the octahedral position of Co^{2+} ions.

The cation distribution was also tested by calculation of lattice parameters from tetrahedral and octahedral Me–O bond distances listed by Poix (15, 16). Using the invariant character of the ‘‘cation–anion’’ distance Poix established the equation

$$a = 2.0995 d_{tet} + [5.8182(d_{oct})^2 - 1.4107(d_{tet})^2]^{1/2},$$

which should be valid for all Sp-type structures. This equation was first tested on the parent $Zn_{2.333}Sb_{0.667}O_4$

spinel. It was found that the Sb–O distance given by Poix (0.1895 nm) is too short. In order to obtain better agreement between the observed and calculated a -value we used 0.1980 nm for the Sb–O bond distance [which actually is the sum of Shannon's ionic radii for Sb(V) and O^{2-}]. Then the lattice parameters for all synthesized spinels were calculated given the assumption that the tetrahedral site is occupied exclusively by Zn^{2+} ions. It can be seen from data listed in Table 1 that the differences between a_{obs} and a_{calc} are in the most cases less than 0.001 nm (a maximum value is 0.0017 nm).

As a consequence of the strong octahedral preferences of Cr^{3+} and Mn^{3+} ions the corresponding tetrahedral Me³⁺–O distances are not known. Therefore, the other possible Me cation distribution, $(Me_yZn_{1-y})[Zn_{x-1+y}Sb_z]O_4$, was tested only for Co and Ni spinels. The calculated a -values for all Ni spinels are identical (Table 1), which is not in agreement with the experimental values. As stated above the radii of Zn^{2+} and Co^{2+} ions are very close and the calculated a -values for different cation distributions are very similar. This means that the choice between different cation distributions is possible only from the results of XRD data.

The results presented strongly support supposed cation distribution $(Zn_1)[Zn_{x-1}Me_ySb_z]O_4$. The fact that lattice parameters depend linearly on spinel composition also confirms the same cation distribution within each series.

CONCLUDING REMARKS

These results enable the use of the curves in Fig. 1 for the characterization of $Zn_{2.333}Sb_{0.667}O_4$ spinel doped with various Me ions (Me = Cr, Mn, Co, or Ni). By assuming that the contribution of each ionic species to the lattice parameter of resulting Sp phases is additive, it could be possible to estimate lattice constants of more complex spinels with similar composition. For example, the estimated value for $Zn_{1.991}Ni_{0.090}Co_{0.030}Cr_{0.247}Mn_{0.090}Sb_{0.545}O_4$ spinel (0.8547 nm) is in excellent agreement with the experimental value (Table 1). We suppose that with a known composition of initial varistor mixture and an experimentally determined lattice constant of resulting Sp phase in sintered material, it will be possible to estimate the

composition of Sp phase. This will be the object of our future studies.

REFERENCES

1. W. Büchner, R. Schliebs, G. Winter, and K. H. Büchel, "Industrial Inorganic Chemistry," p. 543. VCH Verlagsgesellschaft, Weinheim, 1989.
2. A. R. West, "Solid State Chemistry and Its Applications," p. 569. Wiley, Chichester, 1984.
3. W. Büchner, R. Schliebs, G. Winter, and K. H. Büchel, "Industrial Inorganic Chemistry," p. 432. VCH Verlagsgesellschaft, Weinheim, 1989.
4. G. Delpiero, F. Trifiro, and A. Vaccari, *J. Chem. Soc. Chem. Commun.* 656, (1984).
5. Z. Kowalczyk and S. Jodzis, *Appl. Catal.* **58**, 29 (1990).
6. T. Asokan and R. Freer, *J. Mater. Sci.* **25**, 2447 (1990).
7. J. Wong, *J. Appl. Phys.* **51**, 4453 (1980).
8. J. P. Mah, J. S. Choi, and S. H. Peak, *J. Mater. Sci.* **25**, 3375 (1990).
9. T. Takemura, M. Kobayashi, Y. Takada, and K. Sato, *J. Am. Ceram. Soc.* **69**, 430 (1986).
10. M. Inada, *Jpn. J. Appl. Phys.* **17** (1978) 1.
11. K.-H. Bäther, D. Hinz, N. Mattern, M. Bitterlich, and W. Brückner, *Phys. Status Solidi A* **61**, K9 (1980).
12. M. Inada, *Jpn. J. Appl. Phys.* **19**, 409 (1980).
13. R. J. Hill, J. R. Craig, and G. V. Gibbs, *Phys. Chem. Miner.* **4**, 317 (1979).
14. R. D. Shannon, *Acta Crystallogr. Sect. A* **32**, 751 (1976).
15. P. Poix, *Bull. Soc. Chim. Fr.* **5**, 1085 (1965).
16. P. Poix, *C. R. Acad. Sci. Paris Ser. C* **268**, 1139 (1969).
17. R. G. Garvey, *Powder Diffr.* **1**, 114 (1986).
18. H. M. Rietveld, *J. Appl. Crystallogr.* **2**, 65 (1969).
19. A. Sakthivel and R. A. Young, School of Physics, Georgia State Univ. Atlanta.
20. O. Knop, K. I. G. Reid, Sutarno, and Y. Nakagawa, *Can. J. Chem.* **46**, 3463 (1968).
21. H. Kasper, *Monatsh. Chem.* **98**, 1207 (1967).
22. Joint Committee on Powder Diffraction Standards, International Center for Diffraction Data, Swarthmore, USA.
23. H. St. C. O'Neill and A. Navrotsky, *Am. Miner.* **68**, 181 (1983).
24. F. A. Cotton, G. Wilkinson, "Advanced Inorganic Chemistry," 5th Ed., p. 594. Wiley, New York, 1988.
25. A. Navrotsky and O. J. Kleppa, *J. Inorg. Nucl. Chem.* **29**, 2701 (1967).
26. H. St. C. O'Neill and A. Navrotsky, *Am. Miner.* **69**, 733 (1984).
27. V. S. Urusov, *Phys. Chem. Miner.* **9**, 1 (1983).
28. F. A. Cotton, G. Wilkinson, "Advanced Inorganic Chemistry," 5th Ed., p. 686. Wiley, New York, 1988.
29. F. A. Cotton, G. Wilkinson, "Advanced Inorganic Chemistry," 5th Ed., p. 430. Wiley, New York, 1988.
30. C. P. Marshall and W. A. Dollase, *Am. Miner.* **69**, 928 (1984).
31. P. G. Casado and I. Rasines, *Polyhedron* **4**, 517 (1985).